Available online at www.sciencedirect.com
ScienceDirect
Atmospheric Environment 42 (2008) 2849–2863
ATMOSPHERIC ENVIRONMENT
www.elsevier.com/locate/atmosenv

Assessing the photochemical impact of snow NO_x emissions over Antarctica during ANTCI 2003 ☆

Yuhang Wang[a,*], Yunsoo Choi[a], Tao Zeng[a], Douglas Davis[a], Martin Buhr[b], L. Gregory Huey[a], William Neff[c]

[a]*Georgia Institute of Technology, Atlanta, GA 30332, USA*
[b]*Air Quality Design, Golden, CO 80403, USA*
[c]*NOAA Earth System Research Laboratory, Physical Sciences Division, Boulder, CO 80305, USA*

Received 21 July 2006; received in revised form 22 January 2007; accepted 23 January 2007

Abstract

Surface and aircraft measurements show large amounts of reactive nitrogen over the Antarctic plateau during the ANTCI 2003 experiment. We make use of 1-D and 3-D chemical transport model simulations to analyze these measurements and assess the photochemical impact of snow NO_x emissions. Boundary layer heights measured by SODAR at the South Pole were simulated reasonably well by the polar version of MM5 after a modification of ETA turbulence scheme. The average of model-derived snow NO_x emissions ($3.2-4.2\times10^8$ molec cm^{-2} s^{-1}) at the South Pole is similar to the measured flux of 3.9×10^8 molec cm^{-2} s^{-1} during ISCAT 2000. Daytime snow NO_x emission is parameterized as a function of temperature and wind speed. Surface measurements of NO, HNO_3 and HNO_4, and balloon measurements of NO at the South Pole are reasonably simulated by 1-D and 3-D models. Compared to Twin Otter measurements of NO over plateau regions, 3-D model simulated NO concentrations are at the low end of the observations, suggesting either that the parameterization based on surface measurements at the South Pole underestimates emissions at higher-elevation plateau regions or that the limited aircraft database may not be totally representative for the season of the year sampled. However, the spatial variability of near-surface NO measured by the aircraft is captured by the model to a large extent, indicating that snow NO_x emissions are through a common mechanism. An average emission flux of 0.25 kg N km^{-2} month^{-1} is calculated for December 2003 over the plateau (elevation above 2.5 km). About 50% of reactive nitrogen is lost by deposition and the other 50% by transport. The 3-D model results indicate a shallow but highly photochemically active oxidizing "canopy" enshrouding the entire Antarctic plateau due to snow NO_x emissions.

Keywords: Antarctica; Photochemistry and transport; Snow emissions; Nitrogen flux; ANTCI

1. Introduction

Previous investigation of sulfur chemistry in the antarctic troposphere (ISCAT) experiments in 1998 and 2000 revealed high concentrations of NO at the South Pole (SP). The NO mixing ratios reached over 500 pptv (Davis et al., 2001, 2004), considerably

Doi of original article: 10.1016/j.atmosenv.2007.01.056
☆ This paper was inadvertently published in a regular issue, it is therefore being republished in the correct place within this special issue.
*Corresponding author.
E-mail address: ywang@eas.gatech.edu (Y. Wang).

1352-2310/$ - see front matter © 2008 Elsevier Ltd. All rights reserved.
doi:10.1016/j.atmosenv.2007.07.062

higher than what was seen in the Arctic (e.g., Honrath et al., 1999; Ridley et al., 2000). The emissions of NO_x result from nitrate photolysis inside snow pack (Davis et al., 2001 and references therein). At SP, measurements show 24-h average concentrations of OH higher than in the tropical marine boundary (Mauldin et al., 2001, 2004). Active photochemistry driven by snow NO emissions lead to significant ozone production (e.g., Crawford et al., 2001; Chen et al., 2004). Davis et al. (2004) have further speculated that given the rate of nitrate photolysis most of the plateau should exhibit high levels of ozone as well as OH near the surface.

What remains unclear are the spatial extent and the overall impact of snow NO_x emissions on photochemistry over Antarctica. Flux estimates by Jones et al. (2001) at the German Antarctic station, Neumayer (70°S, 8°W), are only about $\frac{1}{3}$ of the flux estimated by Oncley et al. (2004) at SP. Clearly snow emissions vary over Antarctica. To begin addressing the many issues related to reactive nitrogen and its coupling to atmospheric oxidizing species such as OH, we need to extend the measurements of NO_x to include a larger area of Antarctica and extend previous box model analysis to 1-D and 3-D analyses.

The Antarctic Tropospheric Chemistry Investigation (ANTCI) took place in late November and December 2003 (Eisele et al., this issue). Compared to the ISCAT 1998 and 2000 studies, tethered balloon observations at SP (Helmig et al., this issue) along with plateau measurements by a Twin Otter aircraft provided, for the first time, some critical spatial information of NO over Antarctica (Davis et al., this issue). To analyze these and SP surface measurements, we have applied 1-D and regional 3-D chemical transport models. The 1-D model is applied to construct a snowpack NO_x emission parameterization and 1-D model simulations are used to investigate the effects of vertical transport on reactive nitrogen on the basis of SP measurements. The snowpack NO_x emission parameterization is implemented in the 3-D model to examine the effects of transport by advection and the spatial heterogeneity of snowpack NO_x emissions on the basis of balloon and Twin Otter measurements. Our modeling analysis focuses specifically on the plateau region where the highest emission rates of NO_x are thought to occur. We describe the models in Section 2. We construct a snow NO_x emission parameterization to enable 3-D modeling in Section 3. Evaluations of 1-D and 3-D model simulations with surface measurements of reactive nitrogen are discussed in Section 4. Finally, we compare our model simulations with balloon and Twin Otter measurements and assess the impact of snow NO_x emissions on reactive nitrogen budget and photochemistry over Antarctica in Section 5. Conclusions are given in Section 6.

2. 3-D model descriptions and 1-D model setup

The regional 3-D modeling system has two components, the polar version of the Penn State/National Center for Atmospheric Research mesoscale model MM5 and a regional chemistry and transport model. The models have a horizontal spatial resolution of $80 \times 80\,km^2$. There are 27 vertical layers up to 10 hPa, 13 of which are placed in the lowest 1 km in order to simulate the vertical distribution of trace gases in the boundary layer. In our simulations, the MM5 simulation domain is 5 grid boxes larger on each side than the chemical transport simulation domain such that any dynamic anomaly near the boundary does not affect transport in the chemical model.

We use the polar version of MM5 (Bromwich et al., 2001; Cassano et al., 2001), which provides better meteorological simulations in comparison to regular MM5 or other similar models because the model has specific physical parameterizations for polar regions. In our simulations over Antarctica, we use 4-D data assimilation conducted with the ECMWF reanalysis, rawinsonde and surface observations. Most meteorological data are archived every 30 min. We archive turbulence statistics every 2.5 min in order to resolve the turbulent transport in the boundary layer. We use the ETA Mellor-Yamada-Janjic (MYJ) 2.5-order closure scheme (Black, 1994) for the turbulence calculation.

The regional chemical transport model (Zeng et al., 2003, 2006; Choi et al., 2005; Wang et al., 2006; Jing et al., 2006) adopts the photochemical and dry and wet deposition modules from the GEOS-CHEM model (Bey et al., 2001). The model includes a detailed photochemical mechanism with about 200 reactions and 120 concentration-varying chemical species; 24 tracers (family or species) are transported to describe O_3-NO_x–hydrocarbon chemistry. Recent kinetics data on HNO_4 photolysis and thermal decomposition (Roehl et al., 2002; Gierczak et al., 2005) are used in this work. The transport scheme is that by Walcek (2000). We apply the simulation results of the global GEOS-CHEM model to specify initial and daily boundary

conditions of trace gas concentrations in the regional model. GEOS-CHEM (version 5.02, 4° latitude × 5° longitude resolution) is driven by GEOS-4 assimilated fields for 2003 by the NASA Global Modeling and Assimilation Office.

A 1-D model derived from the 3-D model with vertical transport only by turbulence is used to analyze the interaction of snow NO_x emissions, photochemistry, dry deposition, and turbulent transport in the boundary layer at SP. The 1-D and 3-D models therefore share the same vertical structure and meteorological fields (for SP in the 3-D model). GEOS-CHEM results are used for initial and upper chemical boundary condition at 1 km in 1-D simulations, which is well above the shallow atmospheric boundary layer at SP (Neff et al., this issue). A specific objective of the 1-D simulations is to construct, on the basis of SP measurements, a parameterization of snow NO_x emissions that can be used in the 3-D model for Antarctica. We use the 1-D model for this purpose because the iterative 1-D NO_x flux analysis detailed in the next section cannot be executed within the 3-D model. We chose not to include snow emissions of H_2O_2 and CH_2O (Hutterli et al., 2004) in this work for three reasons. First, measurements of H_2O_2 at the SP show similar magnitudes (~270 pptv) to those in 2000 reported by Hutterli et al. (2004). However, CH_2O mixing ratios (20–60 ppbv) are lower than values in 2000 (50–150 ppbv). Model simulations for ANTCI 2003 constrained by observed concentrations of O_3, NO, hydrocarbons, and water vapor and photolysis rates of $J(O^1D)$ and $J(NO_2)$ show CH_2O values in the range of the 2000 measurements (50–120 ppbv) but higher than 2003 measurements, implying a photochemical sink for CH_2O in snow rather than a source during ANTCI 2003. Second, measurements of H_2O_2 in 2003 are fairly constant (~200 ppbv higher than model results). We are unable to parameterize the diagnosed emissions as functions of other variables as we did with snow NO_x emissions. Without H_2O_2 measurements in other regions, we cannot extend the emissions to other regions of Antarctica in the 3-D model. Lastly, as discussed by Chen et al. (2004), the photochemical model (without snow emissions of H_2O_2) overestimates OH measurements. Similar discrepancies were found in the 2003 experiment. Inclusion of snow H_2O_2 emissions will further increase the model overestimates. More targeted measurements will be needed to resolve the disagreement between simulated and measured OH (Chen et al., 2004). We will take this uncertainty into consideration when analyzing 3-D model results but will not discuss further the model-measurement comparisons in regard to HO_x chemistry, which would largely be a duplication of the work by Chen et al. (2004).

3. Snow NO_x emission flux parameterization

We apply the 1-D model to estimate the snow NO_x emissions based on trace gas measurements at SP. We assume that the emissions are in the form of NO_2 (Jones et al., 2000). Davis et al. (2004), however, showed that at the surface NO and NO_2 are in photochemical equilibrium based on measurements taken at −20 cm to the surface. Whether the emissions are in the form of NO or NO_2 does not change the simulation results because these species reach photochemical equilibrium in minutes in the plateau atmosphere with the amount of O_3 present. We first compare simulated meteorological variables to the measurements at SP.

3.1. Effects of turbulence on boundary layer height and surface temperature and wind speed

A key measurement pertinent to the model flux estimation is that of boundary layer height estimated using the Sound Detection And Ranging (SODAR) instrument. Based on the backscattered signals (due to boundary layer turbulence structures), an automatic algorithm (Neff et al., this issue) was applied to identify the boundary layer height. The maximum range of the instrument as configured for the ANTCI 2003 study was 180 m. The simulated diffusion coefficient drops rapidly to the minimum value at the top of the boundary layer. Therefore we define the boundary layer height in the model as the altitude at which the turbulence diffusion coefficient drops to a value equivalent to 10 times of the minimum value specified in the model. Based on this approach, the polar MM5 simulation using the original ETA MYJ 2.5-order closure scheme clearly underestimates SODAR measurements since the boundary layer only occasionally extends beyond the first model layer (Fig. 1). Further analysis reveals a problematic assumption in the MM5 MYJ turbulence scheme implementation, i.e., the default minimum diffusion coefficient is set at $0.09\,m^2\,s^{-1}$. While a reasonable minimum value for mid-latitude North America, it is too high over the polar region, where surface roughness of snow is very low. Thus, we decreased

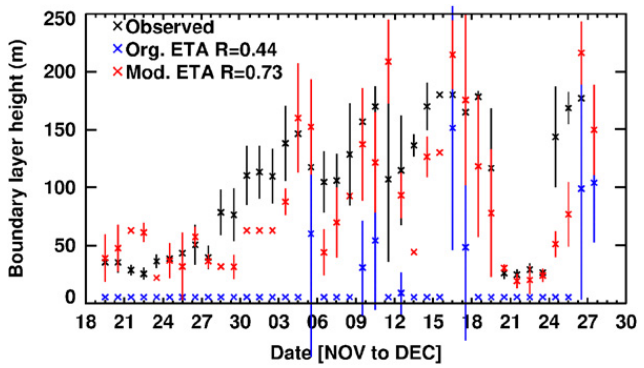

Fig. 1. Observed and simulated daily boundary layer heights at SP during ANTCI 2003. Simulation results using the original and modified ETA MYJ turbulence schemes are shown. The vertical bar shows daily standard deviation. The maximum altitude measurable by SODAR is 180 m.

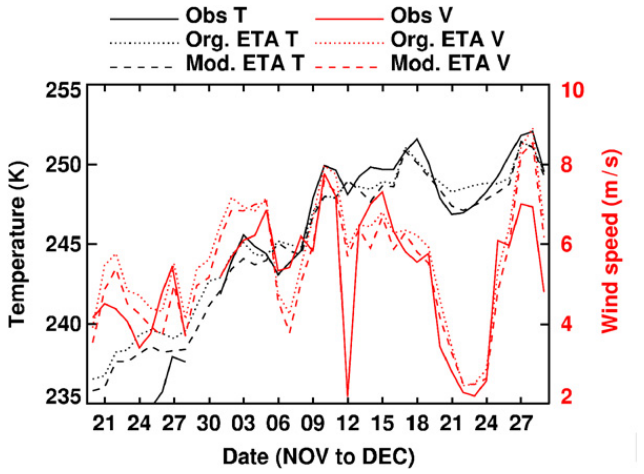

Fig. 2. Same as Fig. 1 but for temperature and wind speed. "T" denotes temperature and "V" denotes wind speed.

the minimum value to $0.001\,m^2\,s^{-1}$.With this adjustment, the simulated boundary layer height is much higher and in reasonable agreement with the SODAR measurements, particularly in light of the model's vertical resolution and the uncertainty in the SODAR boundary layer height detection algorithm (Neff et al., this issue). The correlation coefficient between observed and simulated boundary layer heights improves to 0.73 from 0.44.

Simulated surface wind speed and temperature at SP are not strongly affected by the modification of the turbulence scheme (Fig. 2). Some improvement in temperature simulations can be seen. Polar MM5 has a warm bias in late November. When the minimum diffusion coefficient is reduced to $0.001\,m^2\,s^{-1}$, the warm bias is reduced (but not eliminated). Model simulated friction velocity (u_*) values are in good agreement with sonic anemometer measurements in the second half of December (not shown). The surface stress simulation is not significantly affected by changing the minimum diffusion coefficient in the model. Additional evidence was found in our recent model analysis of (halogen-driven) ozone depletion events at Alert, Canada, in which the model simulations of surface ozone at Alert were much improved in May when the minimum diffusion coefficient is decreased from 0.09 to $0.001\,m^2\,s^{-1}$ (Zeng et al., 2006). Thus, we adjusted the minimum diffusion coefficient to the lower value for our simulations.

3.2. *Snow NO_x emission flux estimation and parameterization*

We constrain the 1-D model with observed concentrations of O_3, hydrocarbons, and water vapor and photolysis rates of $J(O^1D)$ and $J(NO_2)$. Trace gas measurements were made on the second floor of the Atmospheric Research Observatory (ARO), approximately 10 m above the snow surface. The presence of the ARO building induces local-scale mixing; we therefore consider these measurements as averages for the lowest model layer (0–10 m). All measurements have higher measurement frequencies than $hour^{-1}$; hourly averages are used in model analyses. The surface NO_x concentrations in the model are determined by an influx from the snow pack, an outflux to higher altitudes, and chemical production and loss. Other than the snow emission flux, all other terms are calculated in the 1-D model. With measurements of NO, we can therefore derive snow NO_x emission fluxes using the model. Our initial guess of the snow emission is 3.9×10^8 molec $cm^{-2}\,s^{-1}$ (Oncley et al., 2004). This emission flux is adjusted iteratively until model simulated surface NO concentrations match the measurements (to $<1\%$ each hour) or if the flux is reduced to 0. The derived daily snow NO_x flux is shown in Fig. 3.The average emission flux derived from the 1-D model is 3.2×10^8 molec $cm^{-2}\,s^{-1}$, which is 20% lower than the mean flux of 3.9×10^8 molec $cm^{-2}\,s^{-1}$ estimated by Oncley et al. (2004) using sonic anemometer/thermometers and NO measurements in late November/early December during the ISCAT 2000 study. The reasonable agreement between NO_x flux estimates for ISCAT 2000 and ANTCI 2003 could be fortuitous. Additional flux measurements/model analyses are needed to provide more substantial constraints on the year-to-year variability of snow emissions at the site.

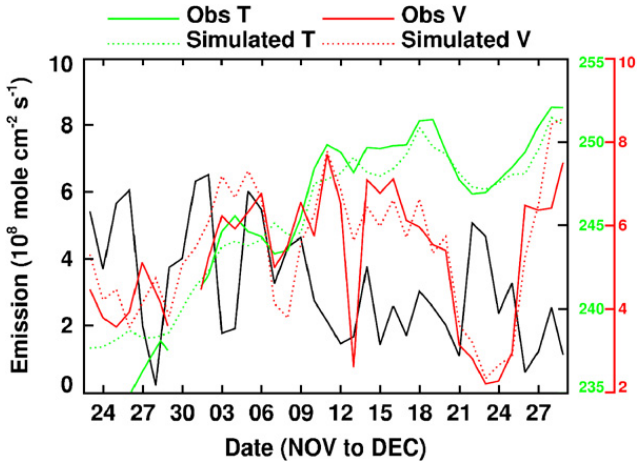

Fig. 3. 1-D model derived daily snow NO_x emissions, observed and simulated temperature and wind speed at SP. The black line shows model derived snow NO_x emissions. "T" denotes temperature (K) and "V" denotes wind speed ($m\,s^{-1}$).

Superimposed on the NO_x flux in Fig. 3 are observed and simulated temperature and wind speed. The derived flux appears to show anti-correlations with temperature and to some extent with wind speed. Other variables, such as surface pressure and humidity, do not significantly correlate or anti-correlate with the derived NO_x flux. Here we parameterized on a daily basis the emission flux as polynomials of simulated wind speed and temperature up to the second order and obtained,

$$NO_x\ \text{flux} = -1009 + 8.38T - 0.0173T^2 + 2.008v + 0.0689v^2 - 0.011vT, \quad (1)$$

where the flux is in 10^8 molec $cm^{-2}\,s^{-1}$, temperature T in K, and wind speed v in $m\,s^{-1}$. Fig. 4 shows the parameterized flux as a function of temperature at a wind speed of $5\,m\,s^{-1}$ and as a function of wind speed at a temperature of 245 K. We see that the derived snow NO_x emission tends to increase with decreasing temperature; but the rate of change is higher at the high temperature end. By comparison, the flux dependence on wind speed is relatively weak and nonlinear. Generally speaking, the derived snow emission rate tends to increase with decreasing wind speed at the low end, but tends to increase with increasing wind at the high end. The flux variation with wind speed is relatively small.

The ranges of temperature and wind speed in the parameterization are limited by the measurements at SP (temperature from 238 to 252 K and wind speed from 2 to $9\,m\,s^{-1}$). When applied in the 3-D model, temperature and wind speed can exceed these ranges. We linearly extrapolate the parameterization for temperatures (up to 260 K when flux is >0). The flux dependence on wind speed is weak; we do not use any extrapolation, i.e., out of bound wind speeds are replaced by the respective bound values. We did not find significant correlations of the derived snow NO_x emission flux with ozone column density, solar zenith angle, or values of $J(O^1D)$ or $J(NO_2)$. It appears that the lack of any correlation is due in part to the relatively small range of values for these photochemical parameters at SP. Emissions of NO_x from the snow pack are allowed only during daylight conditions in the 3-D simulations.

The empirical emission parameterization is constructed here to sidestep the lack of fundamental and quantitative knowledge of the snow NO_x emission process such that measurements from ANTCI 2003 can be analyzed via model simulations to improve our understanding of photochemical processes over Antarctica. As a result, usage of the emission parameterization in other periods may lead to significant errors. A more process based parameterization of snow pack NO_x emission rate should consider, for example, nitrate concentrations in snow (Simpson et al., 2002; Wolff et al., 2002). However, available snow nitrate measurements over Antarctica are currently very limited in space and time (e.g., Kreutz and Mayewske, 1999) and we do not have the necessary measurements to test the structure of snow nitrate distribution as simulated by Wolff et al. (2002). Interestingly, model estimated snow pack NO_x emissions at SP by Wolff et al. (2002) are a factor of 3–4 lower than the measurement by Oncley et al. (2004) during ISCAT 2000 or the derived average flux from this study. The discrepancy highlights the need for additional laboratory and field measurements to constrain the process-based snow pack emission models.

4. Evaluations with surface reactive nitrogen measurements at SP

We apply the derived snow pack NO_x emission parameterization in the 1-D and 3-D models. We compare 1-D and 3-D model simulated NO mixing ratios with the observations at SP in Fig. 5a. Additional input to the 1-D model consisted of surface measurements of O_3, hydrocarbon concentrations, water vapor, and photolysis rates for $J(O^1D)$ and $J(NO_2)$. However, these measurement constraints could not be applied to the 3-D simulations. In the 1-D simulation, snow NO_x

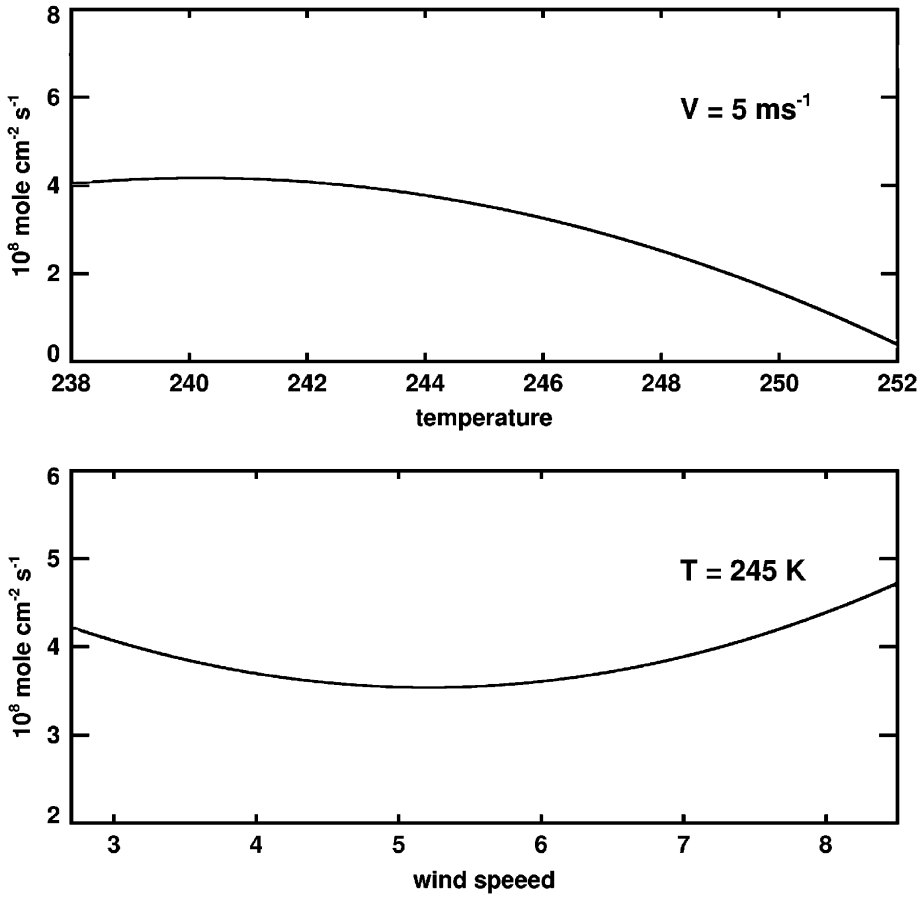

Fig. 4. Parameterized snow pack NO_x emission flux as a function of temperature (K) at a wind speed of 5 m s^{-1} and as a function of wind speed (m s^{-1}) at a temperature of 250 K.

parameterization as a function of temperature and wind speed is used. In the first 3-D simulation, the original model-derived daytime snow emission parameterization is applied over the entire Antarctic continent. In the second 3-D simulation, the parameterized snow emissions are increased by 30%.

The observed high NO episodes on 25, 30 November and 8, 23 December are generally reproduced by the model simulations. Sensitivity results indicate that stable and shallow boundary layers during those periods are main drivers for the developments of high surface NO_x concentrations (Davis et al., 2004). The correlation coefficient between observed and 1-D simulated surface NO concentrations is 0.79. In the 3-D simulation with the original snow NO_x emission parameterization, the model has a tendency to underpredict the observed values; the correlation coefficient is slightly lower at 0.74. Sensitivity analysis indicates that downward advection of lower NO_x concentrations from above in general and horizontal advection of low NO_x air on occasions are key factors in reducing surface NO_x concentrations at SP in the 3-D model compared to 1-D model. The assumption of zero mean vertical and horizontal advection used in eddy correlation measurements and in the 1-D model could be in error because of large-scale downslope katabatic flow over Antarctica. The 3-D model results are improved by increasing snow NO_x emissions by 30%. The increase of NO_x during high NO_x episodes is higher than 30% partly because of the nonlinear relationship between NO_x lifetime and its mixing ratio (Davis et al., 2004). The difference between 1-D and 3-D models indicates a tendency to underestimate snow NO_x emissions by the eddy correlation method, which does not account for advection. All 3-D model results presented hereafter are taken from the simulation with the 30% increase in snow NO_x emissions.

The 3-D model was able to simulate the low NO_x concentrations around 2 December, not captured by the 1-D model. However, the 3-D models clearly underestimate the NO_x episode around 30 November while reproducing the earlier episode around 25 November. Horizontal gradients and transport

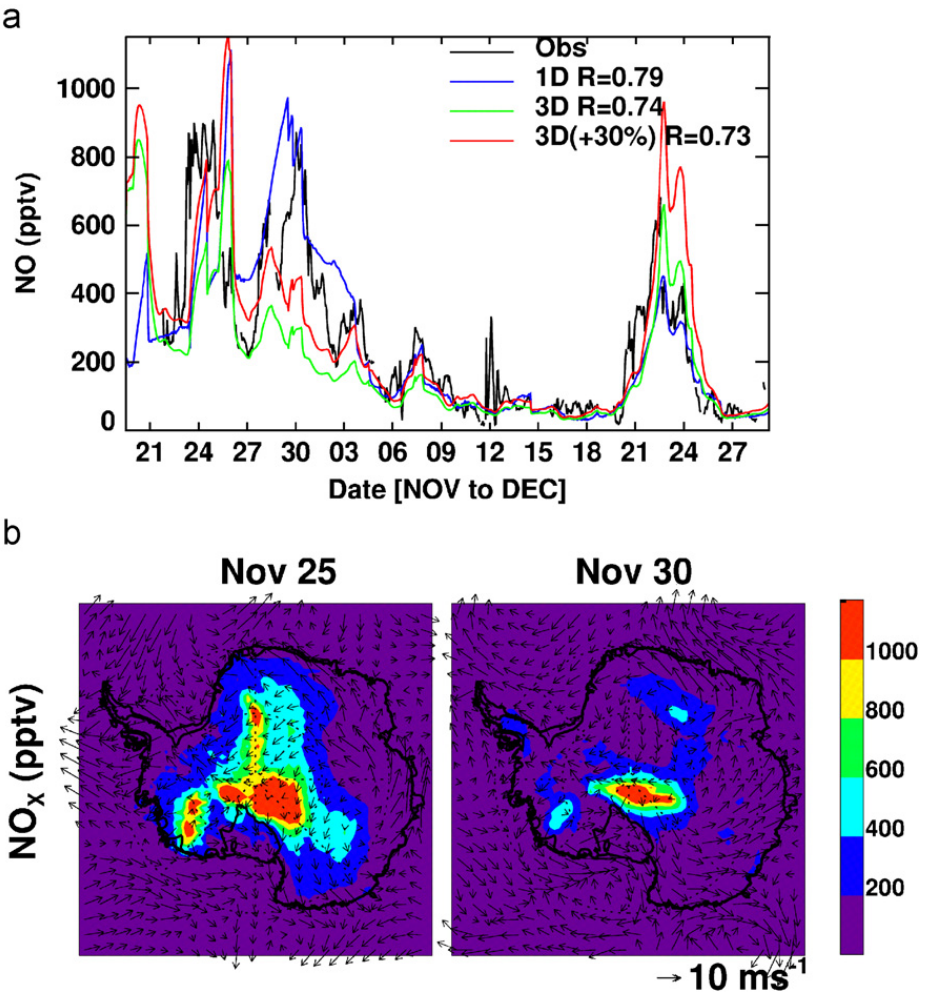

Fig. 5. (a) Observed and 1-D and 3-D model simulated near-surface NO mixing ratios at SP. In the second 3-D simulation, parameterized snow NO_x emissions are increased by 30%. (b) Simulated surface NO_x mixing ratios and wind at 1200 UT on 25 and 30 November, 2003.

appear to play important roles. Fig. 5b compares surface NO_x concentrations and wind transport over Antarctica between 25 and 30 November (1200 UT). The model predicts more extensive high surface NO_x concentrations on 25 November than 30 November. While the high NO_x distribution is nearly homogeneous around SP on 25 November, a large spatial gradient is simulated around SP on 30 November. Simulated surface winds are in good agreement with ANTCI measurements on 25 November and with Automatic Weather Station (AWS) measurements on 30 November. We use AWS data for the latter day when ANTCI wind measurements were unavailable. Along the 0° meridian, prevailing transport on 25 November is from the high-elevation plateau, where NO_x emissions are high; prevailing transport on 30 November is from a northern low-elevation region, where NO_x emissions are low. Low-NO_x transport is important for the creation of spatial NO gradient around SP on 30 November in the 3-D model. The underestimation in the 3-D model but not 1-D model therefore suggests that this low-NO_x transport is exaggerated in the 3-D model; errors in the snow NO_x emission distribution or wind transport and coarse model spatial resolution are possible reasons.

Fig. 6 shows the comparison between observed and simulated surface HNO_3 at SP. Since HNO_3 concentrations have a strong dependence on NO_x concentrations, model errors in NO will propagate into HNO_3 simulations. To eliminate this error, we added another 1-D simulation, in which surface NO concentrations are specified as observed; snow NO_x emission parameterization is therefore not used in this simulation. The dry deposition velocity in the models is calculated with the resistance-in-series scheme by Wesely (1989). The aerodynamic resistance is computed based on ETA MYJ turbulence output. The snow surface resistance of HNO_3 follows Wesely (1989). The calculated average

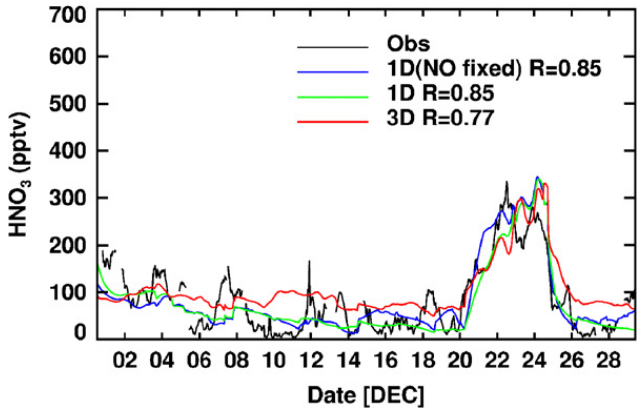

Fig. 6. Same as Fig. 5a but for HNO_3. In the first 1-D simulation, surface NO is specified as observed. In the second 1-D simulation, snow NO_x emission parameterization is used. In the 3-D simulation, parameterized snow NO_x emissions (Eq. (1)) are increased by 30%. The measurement accuracy of HNO_3 is 20% (Huey et al., 2004).

deposition velocity during ANTCI 2003 is $0.15\,cm\,s^{-1}$. The model result shows reasonable agreement with the measurements, revealing low HNO_3 concentrations between 3 and 20 December and high concentrations between 21 and 24 December. The correlation coefficients are 0.85 and 0.77 for 1-D and 3-D models, respectively. Both models tend to overestimate HNO_3 concentrations at low HNO_3 values. However, the 3-D model positive bias is considerably larger; we discuss the reasons after showing the results for HNO_4.

In the HNO_4 simulations, we assume that dry deposition of HNO_4 to snow is as fast as HNO_3 (Slusher et al., 2002). Therefore the average of calculated dry deposition velocities for HNO_4 is $0.15\,cm\,s^{-1}$. Fig. 7 a shows the comparison between observed and simulated HNO_4 at SP. The 1-D simulations are generally in agreement with the measurements except the low bias before 9 December. The observed variability is, however, severely underestimated. The correlation coefficients are 0.63.

In the 1-D model, near-surface HNO_4 is determined by chemical production and loss, turbulent diffusion transport, and dry deposition. We examine each term to investigate which factor is likely the major contributor to the high-frequency variations in the measurements. Fig. 7b shows the time series of each term in December. In this simulation, surface NO is specified as observed. The magnitudes of the four terms are comparable. Chemical production is generally larger than chemical loss; and dry deposition loss is generally larger than turbulent influx from above. During the episode on

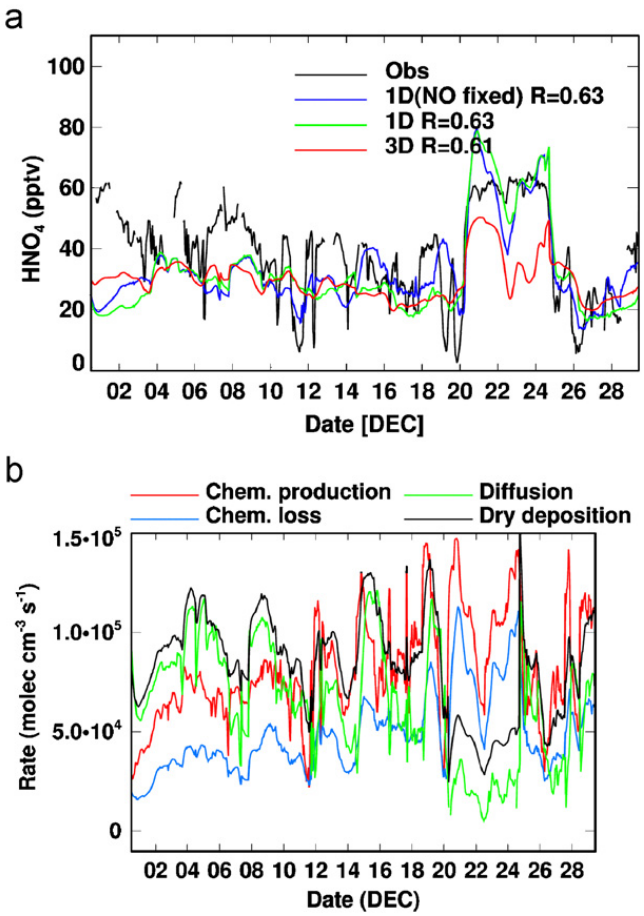

Fig. 7. (a) Same as Fig. 6 but for HNO_4. The measurement accuracy of HNO_4 is 30%. (b) Simulated chemical production, loss, turbulent diffusion transport, and dry deposition rates for HNO_4 near the surface (0–10 m) in the 1-D model.

21–24 December, both turbulent transport and dry deposition are low because of the establishment of a shallow stable boundary layer (Fig. 1). Neither thermal deposition nor photolysis has high-frequency variations. The simulated aerodynamic resistance does not vary in high frequency either. Major portions of high-frequency variations in chemical loss and dry deposition rates are driven by the variability in the simulated HNO_4 concentration. The chemical production rate does have large high-frequency variations, particularly for the period between 12 and 19 December. However, the high-frequency variation is modulated by turbulent transport. The initial large pulse of HNO_4 production is compensated by decrease of turbulent transport from above. If high HNO_4 production driven by snow NO_x emissions continues, production of HNO_4 in the layers above also increases as NO_x is transported upward by turbulence, resulting in accumulation of HNO_4 and an increase of

turbulent influx of HNO_4 to the surface layer. The slower response of the 1-D model simulated HNO_4 to NO variation may indicate that the turbulent transport between the lower model layers is overestimated.

The correlation coefficient between 3-D model simulated and observed HNO_4 is 0.61. The 3-D model simulation is considerably lower than 1-D simulated and measured HNO_4 during the high-concentration episode on 21–24 December. Increasing the snow resistance to HNO_4 deposition decreases dry deposition and increases HNO_4 concentrations. A 50% increase of snow resistance pushes HNO_4 mixing ratios to the upper bound of observed values prior to 20 December, but the model still underestimates on 21–24 December since aerodynamic resistance during this period is high, reducing dry deposition velocity by a factor of 4 from the earlier period. Inspection of the 3-D model results indicates that advection of low HNO_4 to SP on 21–24 December contributes significantly to the low bias in the model.

To further understand the model results, we compare 1-D and 3-D simulated mean vertical profiles of NO, HNO_3, HNO_4 during ANTCI 2003 (Fig. 8). The 1-D simulation with surface NO concentrations specified to the measurements are similar to that with parameterized snow NO_x emissions. Simulated NO profile in the 3-D model are very similar to 1-D profiles despite 30% higher emissions. There is a clear drop off in the NO profiles at about 50 m, around which altitude the boundary layer top resides under stable conditions. The difference between 1-D and 3-D model vertical profiles is much larger for HNO_3 and HNO_4. Both gases show higher values at 50 m than at the surface, suggesting that vertical mixing together with advection might represent an effective loss process for reactive nitrogen from the plateau. It is also noteworthy that both gases have higher estimated concentrations over the altitude range of 50–500 m when calculated using the 3-D than 1-D model. Higher concentrations in 3-D model are driven in part by advection from high plateau regions, a process not simulated in the 1-D model. While not affecting surface HNO_4 concentrations significantly, the accumulation extends to the surface for HNO_3 because of longer chemical lifetimes of HNO_3 than HNO_4. Although model calculated dry deposition is adequate in the 1-D simulations, the overestimates of HNO_3 in the 3-D model indicate a need for lower snow resistance and hence higher HNO_3 deposition. The slightly lower HNO_4 concentration at 0–50 m in the 3-D than 1-D model is due in part to the underestimation during the episode on 21–24 December.

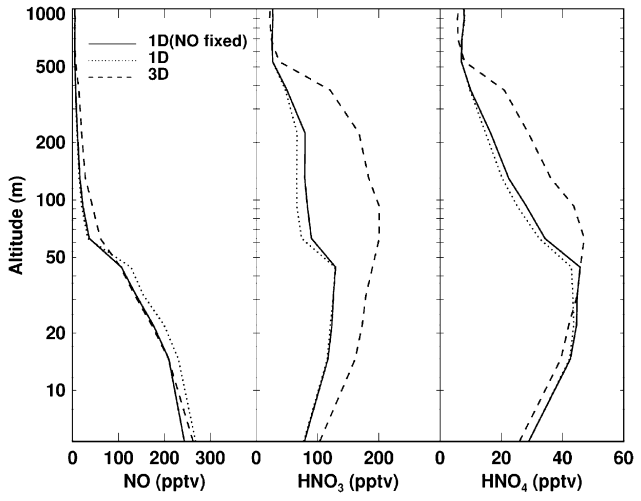

Fig. 8. 1-D and 3-D models simulated mean vertical profiles of NO, HNO_3, and HNO_4 during ANTCI 2003. In the first 1-D simulation, surface NO is specified as observed. In the second 1-D simulation, snow NO_x emission parameterization is used.

Slusher et al. (2002) estimated that HNO_3 and HNO_4 lifetimes against deposition are 3.5 h using box model analysis of ISCAT 2000 measurements. A similar calculation using ANTCI data results in a dry deposition lifetime of 10 h. Slower dry deposition during ANTCI likely reflects a different meteorological environment from ISCAT 2000. Scaling a boundary layer depth to 50–100 m with a deposition velocity of 0.15 cm s^{-1} yields a lifetime in the range of 9–18 h. We note that a simple scaling of boundary layer height with dry deposition velocity underestimates the deposition lifetime of HNO_4 because its concentrations increase by a factor of 2 in the boundary layer (Fig. 8). Estimating dry deposition lifetimes using a box model is reasonable in a well-mixing boundary layer but it is problematic over Antarctica because the boundary layer is frequently stable. The large vertical gradients of HNO_4 and NO_x, which have opposite trends, cannot be taken into account properly in a box model. Furthermore, Fig. 7b shows that diffusion influx is as important as chemical production or deposition loss. In a shallow box near the surface, a box-model calculation would overestimate the loss by dry deposition because it accounts for both dry deposition and diffusion influx. However, the finding by Slusher et al. (2002) that HNO_4 deposition accounts for a significant portion of nitrogen deposition to snow is still valid

in our results since the deposition flux is the product of deposition velocity and trace gas concentration. The deposition velocities are the same for HNO_3 and HNO_4 and their concentrations are in comparable ranges.

5. Comparison with balloon and aircraft NO measurements and assessments of plateau reactive nitrogen budget and photochemical impact over Antarctica

We extend the comparison of model simulated reactive nitrogen with surface measurements to include vertical distributions of NO as recorded by the tethered balloon platform at SP (Helmig et al., this issue) and the Twin Otter data recorded within 400 km of SP but still over the plateau (Davis et al., this issue). For this purpose, the construction of a rather crude empirical daytime snow NO_x emission parameterization (Section 3.2) is critically important, without which it will be difficult to simulate the spatial variability of surface NO_x over Antarctica.

Tethered balloons were used to measure NO vertical distributions at SP on 17–28 December (Fig. 9). High NO_x concentrations were measured near the surface on 21 and 23 December (Fig. 5a); we separate these data from the periods of 17–20 and 25–28 December. During the high-NO_x period of 21 and 23 December (no balloon measurements were made on 24 December), simulated median values at low altitudes are lower than the measurements because of the model underestimation on 21 December (Fig. 5a). The observed and simulated means are closer. The observed decrease of NO with altitude is simulated by the models. During the low-NO_x periods, the simulated median values are too low; the agreements for mean values are better,

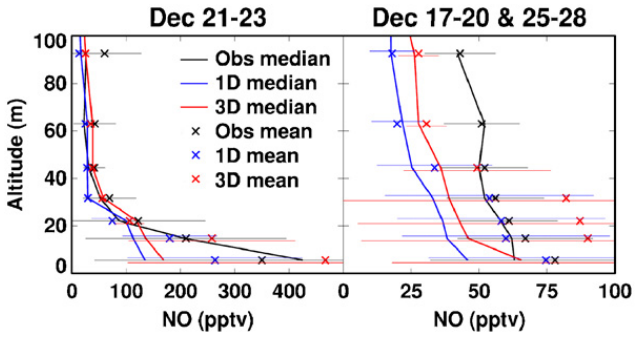

Fig. 9. Balloon measurements of NO profiles on 17–28 December and the corresponding model results. Horizontal bar shows the standard deviation. There are six profiles for 21–23 December and 21 profiles for 17–20 and 25–28 December.

although the low bias is still evident above 60 m. The concentrations in the 3-D model are higher than 1-D model due in part to the 30% higher emissions, and are in better agreement with the observations.

The spatial distribution of NO mixing ratios measured by the Twin Otter at 20–60 m above the surface on 4–6 December are shown in Fig. 10a. From here it can be seen that the observed NO concentrations tend to be higher at higher elevations. Such a spatial distribution is captured by the model simulation. However, the model has a clear low bias. The low bias is also shown in the vertical distribution (Fig. 10b). While the measurements show NO mixing ratios up to 550 pptv, the model results reach only 350 pptv. Surface measurements of 100–200 pptv at SP on 4–6 December are also underestimated by the 3-D model although to a less extent (Fig. 5a). The model simulated emission variability is driven mostly by temperature (Fig. 4); thus, the colder temperatures at higher elevation lead to more NO_x emissions, and hence, higher NO concentrations. The resulting spatial gradient/variability is, however, underestimated by the model. There could be important factors not accounted for in the parameterization, which contribute significantly to the spatial variability of snow NO_x emissions. More extensive spatial and temporal aircraft measurements to improve on their ''representativeness'' as well as detailed laboratory studies of the nitrate photochemical mechanism are needed to adequately evaluate this issue.

The comparison of model simulations with the measurements from the ANTCI 2003 experiment demonstrates that the 3-D model can capture some of the essential features of the airborne data. Given this level of agreement, we applied the 3-D model to explore the reactive nitrogen budget over the plateau and the photochemical impact of snow NO_x emissions over the entire Antarctic continent. The simulated low-altitude NO_x concentrations in general have low biases at SP during low-NO_x periods of balloon measurements and over the plateau regions sampled by Twin Otter, implying that the simulated nitrogen source and photochemical impact (in terms of OH concentrations) may have low biases.

Using the 3-D model results, we construct the nitrogen budget for the plateau region (elevation above 2.5 km). For December 2003, we estimate an emission of 0.25 kg N km^{-2} $month^{-1}$. The reactive nitrogen deposition flux is 0.13 kg N km^{-2} $month^{-1}$.

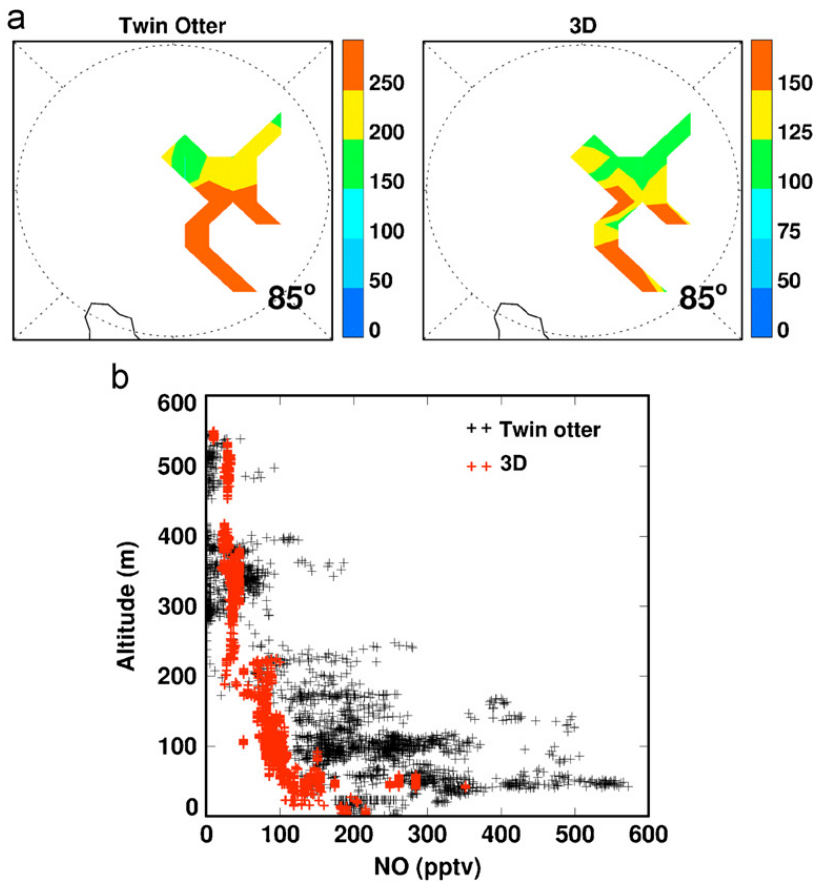

Fig. 10. (a) Comparison of Twin Otter observed and model simulated NO distributions. (a) NO mixing ratios (pptv) at 20–60 m above the surface on 4–6 December. (b) Vertical distributions of NO on 4–6 December. Model results are sampled along flight tracks at the time of measurements.

Depositions of HNO_3 and HNO_4 account for 73% and 21%, respectively, and the rest is largely deposition of NO_2. The net outflux of reactive nitrogen is 0.12 kg N km^{-2} $month^{-1}$. About 90% of the outflux takes place within 1 km above the surface. Outfluxes of HNO_3 and NO_x account for 61% and 26%, respectively, and the rest is mostly HNO_4. Fig. 11 shows the near-surfacefluxes of HNO_3. As indicated in the figure, most of the transport is over East Antarctica. The implications of the outflux on plateau nitrogen chemistry are discussed by Davis et al. (this issue).

Fig. 12 shows model simulated surface NO_x and OH concentrations over Antarctica during the ANTCI 2003 period. The emission parameterization predicts higher NO_x emissions and hence concentrations over the East Antarctic plateau. The concentration of OH does not maximize in regions having the highest NO_x concentrations because of the nonlinearity of HO_x chemistry (Chen et al., 2001, 2004; Davis et al., 2004). Thus, the model predicts some of the highest OH levels in downslope

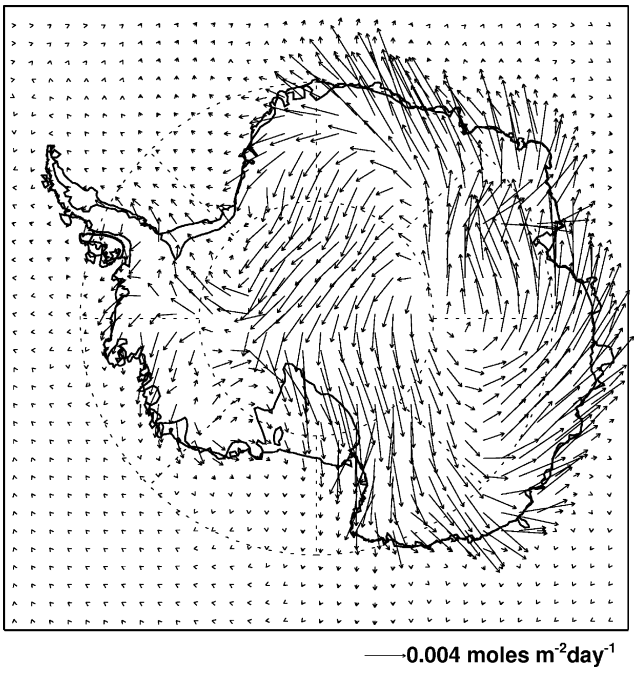

Fig. 11. Simulated monthly mean near-surface HNO_3 fluxes for December 2003.

drainage areas of East Antarctica. Predicted mean surface OH concentrations exceed 2×10^6 molec cm^{-3} over most of the Antarctic continent.

Davis et al. (this issue), using a box model having as its input the Twin Otter plateau NO data set, showed a strong vertical gradient in OH with estimated concentrations reaching as high as 4×10^6 molec cm^{-3}. Based on these results, these authors hypothesized that upon consideration of the likely vertical NO structure across the larger plateau, it is likely that NO_x snow emissions likely lead to an oxidizing canopy that enshrouds the entire plateau. A model simulated cross-section of the OH concentration level along the 90°W–90°E meridian (Fig. 13a) supports their hypothesis, showing a shallow canopy of high OH concentrations above the Antarctic plateau driven by snow NO_x emissions. Fig. 13b shows the simulated distribution of the oxidizing canopy thickness over Antarctica. For illustration purposes, we define the highly active oxidizing canopy as the region with $[OH] \geqslant 3 \times 10^6$ molec cm^{-3}, the highest median value found in the marine boundary over the tropical Pacific (Wang et al., 2001). The simulated OH canopy is deeper over East Antarctic plateau than other regions, generally in the range of 50–150 m. The spatial distribution of the canopy depth reflects a combination of surface NO_x emissions, boundary layer height, and transport.

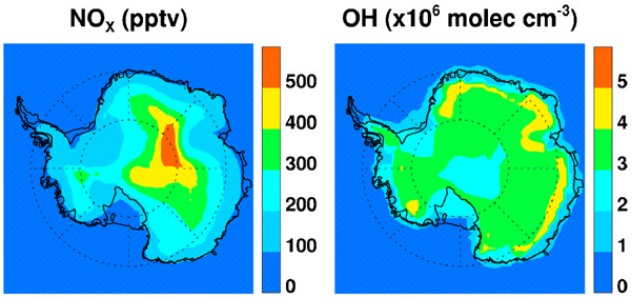

Fig. 12. Simulated mean surface NO_x and OH concentrations during ANTCI 2003.

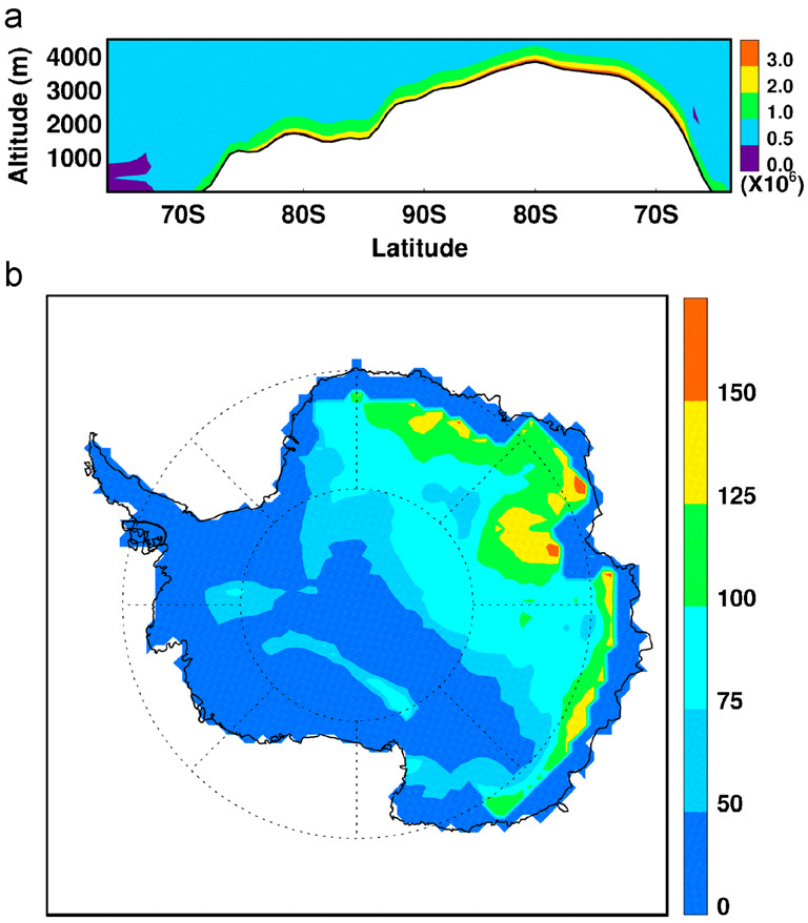

Fig. 13. (a) Simulated cross section of OH concentrations (10^6 molec cm^{-3}) along the 90°W–90°E meridian during ANTCI 2003. (b) Simulated depth (m) of the oxidizing canopy over Antarctica ($[OH] > 3 \times 10^6$ molec cm^{-3}) during ANTCI 2003.

6. Conclusions

We apply 1-D chemistry-diffusion and 3-D chemical transport models to analyze surface, balloon, and aircraft measurements of reactive nitrogen during ANTCI 2003. The emphasis of model analysis is on high NO_x-emitting plateau regions. We simulate the meteorological fields using the polar version of MM5. The default ETA MYJ 2.5-order closure scheme predicts much lower boundary layer heights than SODAR measurements at SP. We decrease the minimum eddy diffusion coefficient from a default value of 0.09 to $0.001\,m^2\,s^{-1}$ and obtain reasonable simulations of SP boundary layer heights.

Using the 1-D chemistry-diffusion model and surface measurements at SP, we derive the necessary snow NO_x emission fluxes that explain the observed NO concentrations. The average emission flux of 3.2×10^8 molec $cm^{-2}\,s^{-1}$ is 20% lower than the mean flux of 3.9×10^8 molec $cm^{-2}\ s^{-1}$ estimated by Oncley et al. (2004) using sonic anemometers, temperature sensors, and high speed NO measurements during ISCAT 2000. We parameterize the derived daytime snow emissions as a function of temperature and wind speed. The empirical parameterization is essential for simulating the spatial variability of observed NO concentrations by Twin Otter. Vertical advection, not accounted for in the 1-D model, decreases surface NO concentrations at SP; daytime snow emissions are increased 30% in the 3-D model to an average of 4.2×10^8 molec $cm^{-2}\,s^{-1}$ at SP in order to reproduce the observed NO concentrations. We calculate an average dry deposition velocity of $0.15\,cm\,s^{-1}$ for HNO_3 and HNO_4 at SP. We find reasonable agreement between observed and simulated HNO_3 and HNO_4 at SP.

To our knowledge, this is first 3-D chemical transport model analysis of reactive nitrogen at SP or over Antarctica in general. Meteorological fields, snow NO_x emission parameterization, and HO_x photochemistry (Chen et al., 2004) all contribute to the overall uncertainties in the simulations. In particular, simulated NO concentrations are too low comparing to Twin Otter measurements during 4–6 December. However, a longer measurement period is needed to assess the representativeness of the bias. Quantifying each of these uncertainties will require much larger data sets than available during ANTCI 2003, and new laboratory studies of the snow nitrate photochemical process. Below, we focus the discussion on two major implications from the model results.

First, inefficient turbulence transport in the relatively stable Antarctic boundary layer leads to large gradients in NO (> a factor of 2 change within the lowest 50 m, Fig. 8), which imply that the vertical structure needs to be simulated to understand photochemistry in the region. For the oxidation products HNO_3 and HNO_4, extensive mixing up to 500 m is simulated. These 1-D vertical profiles are further modified by 3-D transport. The vertical distribution of HNO_3 is affected most. The much longer lifetime of HNO_3 than NO_x or HNO_4 allows for large accumulations of this species in the upper portion of the boundary layer, resulting in significantly higher HNO_3 concentrations near the surface in 3-D than 1-D model. In order to reduce the "excess" HNO_3, the dry deposition velocity of HNO_3 needs to be increased in the 3-D model. Diagnostics using 1-D models will tend to underestimate HNO_3 deposition velocity. While the shape of NO_x vertical profile is not affected by 3-D transport, snow emissions need to be increased by 30% in 3-D model compared to 1-D model. The vertical distribution of HNO_4 is also affected by 3-D transport. Flux measurements of snow emissions or deposition by eddy correlation technique by definition assume zero mean advection of trace gases, which is inconsistent with the prevailing downslope circulation driven by katabatic flow over Antarctica. As a result, the effect of advection needs to be taken into account in the interpretation of any eddy-correlation flux measurements.

Second, the empirical daytime snow NO_x emission parameterization based on temperature and wind speed is obviously an oversimplification of the snow emission process. A more sophisticated process-based emission model that can be coupled with 1-D and 3-D chemical transport models will require additional detailed laboratory studies and more extensive field measurements (particularly by aircraft). Despite the above cited simplifications, the 3-D model has shown that it can capture the observed spatial variability of near-surface NO recorded on the Twin Otter, although the magnitudes are underestimated. These model results suggest that the Antarctic plateau is a major source region for NO_x and that snow NO_x production is through a common mechanism. The model estimates an average NO_x emission flux of $0.25\,kg\,N\,km^{-2}\,month^{-1}$ for December 2003 over the plateau (elevation above 2.5 km). About 50% of

reactive nitrogen is lost by deposition and the other 50% by transport. HNO_3 and HNO_4 are major deposition species (73% and 21%, respectively); nitrogen outflux is largely in form of HNO_3 and NO_x (61% and 26%, respectively). At the simulated NO_x levels, most of the Antarctic continent during ANTCI 2003 has near-surface mean OH concentrations of $>2\times10^6$ molec cm^{-3}. The depth of the layer with [OH] $>3\times10^6$ molec cm^{-3} is estimated to be 50–150 m over the plateau. This result shows a highly photochemically active oxidizing canopy enshrouding the entire Antarctic plateau, which was previously hypothesized by Davis et al. (2004).

Acknowledgements

This work is supported by the National Science Foundation, Office of Polar Programs. We thank Jim Dudhia for his help in modifying the ETA MYJ scheme, Gao Chen for providing the merged data set, Fred Eisele and Jack Dibb for their suggestions, and Robert Yantosca and Daniel Jacob for providing us GEOS-CHEM model and data. The GEOS-CHEM model is managed at Harvard University with support from the NASA Atmospheric Chemistry Modeling and Analysis Program.

References

Bey, I., Jacob, D.J., Yantosca, R.M., Logan, J.A., Field, B., Fiore, A.M., Li, Q., Liu, H., Mickley, L.J., Schultz, M., 2001. Global modeling of tropospheric chemistry with assimilated meteorology: model description and evaluation. Journal of Geophysical Research 106, 23,073–23,096.

Black, T.L., 1994. The new NMC mesoscale ETA model: description and forecast examples. Weather and Forecasting 9, 265–278.

Bromwich, D.H., Cassano, J.J., Klein, T., Heinemann, G., Hines, K.M., Steffen, K., Box, J.E., 2001. Mesoscale modeling of katabatic winds over Greenland with the Polar MM5. Monthly Weather Reviews 129, 2290–2309.

Cassano, J.J., Box, J.E., Bromwich, D.H., Li, L., Steffen, K., 2001. Evaluation of polar MM5 simulations of Greenland's atmospheric circulation. Journal of Geophysical Research 106, 33,867–33,889.

Chen, G., Davis, D., Crawford, J., Nowak, J.B., Eisele, F., Mauldin, R.L., Tanner, D., Buhr, M., Shetter, R., Lefer, B., Arimoto, R., Hogan, A., Blake, D., 2001. An investigation of South Pole HO_x chemistry: comparison of model results with ISCAT observations. Geophysical Research Letters 28 (19), 3633–3636.

Chen, G., Davis, D., Crawford, J., Hutterli, L.M., Huey, L.G., Slusher, D., Mauldin, L., Eisele, F., Tanner, D., Dibb, J., Buhr, M., McConnell, J., Lefer, B., Shetter, R., Blake, D., Song, C.H., Lombardi, K., Arnoldy, J., 2004. A reassessment of HO_x South Pole chemistry based on observations recorded during ISCAT 2000. Atmospheric Environment 38 (32), 5451–5461.

Choi, Y., Wang, Y., Zeng, T., Martin, R., Kurosu, T., Chance, K., 2005. Evidence of lightning NO_x and convective transport of pollutants in satellite observations over North America. Geophysical Research Letters 32, L02805.

Crawford, J.H., Davis, D.D., Chen, G., Buhr, M., Oltmans, S., Weller, R., Mauldin, L., Eisele, F., Shetter, R., Lefer, B., Arimoto, R., Hogan, A., 2001. Evidence for photochemical production of ozone at the South Pole surface. Geophysical Research Letters 28 (19), 3641–3644.

Davis, D., Nowak, J.B., Chen, G., Buhr, M., Arimoto, R., Hogan, A., Eisele, F., Mauldin, L., Tanner, D., Shetter, R., Lefer, B., McMurry, P., 2001. Unexpected high levels of NO observed at South Pole. Geophysical Research Letters 28 (19), 3625–3628.

Davis, D., Chen, G., Buhr, M., Crawford, J., Lenschow, D., Lefer, B., Shetter, R., Eisele, F., Mauldin, L., Hogan, A., 2004. South Pole NO_x chemistry: an assessment of factors controlling variability and absolute levels. Atmospheric Environment 38 (32), 5375–5388.

Davis, D.D., Crawford, J., Chen, G., Wang, Y., Buhr, M., Helmig, D., Blake, D., Neff, W., Eisele, F., this issue. A reassessment of Antarctic plateau reactive nitrogen based on ANTCI 2003 airborne and ground based measurements.

Eisele, F., et al., this issue. An overview of ANTCI 2003. Atmospheric Environment, submitted for publication.

Gierczak, T., Jimenez, E., Riffault, V., Burkholder, J.B., Ravishankara, A.R., 2005. Thermal decomposition of HO_2NO_2 (peroxynitricacid, PNA): rate coefficient and determination of the enthalpy of formation. Journal of Physical Chemistry A 109, 586–596.

Helmig, D., et al., this issue. Nitric oxide in the boundary-layer at South Pole during the Antarctic Tropospheric Chemistry Investigation (ANTCI). Atmospheric Environment, submitted for publication.

Honrath, R.E., Peterson, M.C., Guo, S., Dibb, J.E., Shepson, P.B., Campbell, B., 1999. Evidence of NO_x production within or upon ice particles in the Greenland snowpack. Geophysical Research Letters 26 (6), 695–698.

Huey, L.G., et al., 2004. CIMS measurements of HNO_3 and SO_2 at the South Pole during ISCAT 2000. Atmospheric Environment 38, 5411–5421.

Hutterli, M.A., McConnell, J.R., Chen, G., Bales, R.C., Davis, D.D., Lenschow, D.H., 2004. Formaldehyde and hydrogen peroxide in air, snow and interstitial air at South Pole. Atmospheric Environment 38 (32), 5439–5450.

Jing, P., Cunnold, D., Choi, Y., Wang, Y., 2006. Summertime tropospheric ozone columns from Aura OMI/MLS measurements versus regional model results over the United States. Geophysical Research Letters 33, L17817.

Jones, A.E., Weller, R., Wolff, E.W., Jacobi, H.W., 2000. Speciation and rate of photochemical NO and NO_2 production in Antarctic snow. Geophysical Research Letters 27 (3), 345–348.

Jones, A.E., Weller, R., Anderson, P.S., Jacobi, H.W., Wolff, E.W., Schrems, O., Miller, H., 2001. Measurements of NO_x emissions from the Antarctic snowpack. Geophysical Research Letters 28 (8), 1499–1502.

Kreutz, K.J., Mayewske, P.A., 1999. Spatial variability of Antarctic surface snow glaciochemistry: implications for palaeoatmospheric circulation reconstructions. Antarctic Science 11, 105–118.

Mauldin, R.L., Eisele, F.L., Tanner, D.J., Kosciuch, E., Shetter, R., Lefer, B., Hall, S.R., Nowak, J.B., Buhr, M., Chen, G., Wang, P., Davis, D., 2001. Measurements of OH, H_2SO_4, and MSA at the South Pole during ISCAT. Geophysical Research Letters 28 (19), 3629–3632.

Mauldin, R.L., Kosciuch, E., Henry, B., Eisele, F.L., Shetter, R., Lefer, B., Chen, G., Davis, D., Huey, G., Tanner, D., 2004. Measurements of OH, $HO_2 + RO_2$, H_2SO_4, and MSA at the South Pole during ISCAT 2000. Atmospheric Environment 38 (32), 5423–5437.

Neff, W., Helmig, D., Grachev, A., Davis, D., this issue. A study of boundary layer behavior associated with high NO concentrations at the South Pole using minisodar, tethered balloon, and sonic anemometer. Atmospheric Environment, submitted for publication.

Oncley, S., et al., 2004. Observations of summertime NO fluxes and boundary-layer height at the South Pole during ISCAT 2000 using scalar similarity. Atmospheric Environment, 38, 5389–5398.

Ridley, B., Walega, J., Montzka, D., Grahek, F., Atlas, E., Flocke, F., Stroud, V., Deary, J., Gallant, A., Boudries, H., Bottenheim, J., Anlauf, K., Worthy, D., Sumner, A.L., Splawn, B., Shepson, P., 2000. Is the Arctic surface layer a source and sink of NO_x in winter/spring? Journal of Atmospheric Chemistry 36 (1), 1–22.

Roehl, C.M., Nizkorodov, S.A., Zhang, H., Blake, G.A., Wennberg, P., 2002. Photodissociation of peroxynitricacid in the near-IR. Journal of Physical Chemistry A 106, 3766–3772.

Simpson, R.S., et al., 2002. Radiation-transfer modeling of snowpack photochemical processes during ALERT2000. Atmospheric Environment 36, 2663–2670.

Slusher, D.L., Pitteri, S.J., Haman, B.J., Tanner, D.J., Huey, L.G., 2002. A chemical ionization technique for measurement of pernitric acid in the upper troposphere and the polar boundary layer. Geophysical Research Letters 28 (20), 3875–3878.

Walcek, C.J., 2000. Minor flux adjustment near mixing ratio extremes for simplified yet highly accurate monotonic calculation of tracer advection. Journal of Geophysical Research 105, 9335–9348.

Wang, Y., et al., 2001. Factors controlling tropospheric O_3, OH, NO_x, and SO_2 over the tropical Pacific during PEM-tropics B. Journal of Geophysical Research 106, 32,733–32,748.

Wang, Y., Choi, Y., Zeng, T., Ridley, B., Blake, N., Blake, D., Flocke, F., 2006. Late-spring increase of trans-Pacific pollution transport in the upper troposphere. Geophysical Research Letters 33, L01811.

Wesely, M.L., 1989. Parameterization of surface resistance to gaseous dry deposition in regional-scale numerical models. Atmospheric Environment 23, 1293–1304.

Wolff, E.W., Jones, A.E., Martin, T.J., Grenfell, T.C., 2002. Modelling photochemical NO_x production and nitrate loss in the upper snowpack of Antarctica. Geophysical Research Letters 29, 1944.

Zeng, T., Wang, Y., Chance, K., Browell, E.V., Ridley, B.A., Atlas, E.L., 2003. Widespread persistent near-surface ozone depletion at northern high latitudes in spring. Geophysical Research Letters 30, 2298.

Zeng, T., Wang, Y., Chance, K., Blake, N., Blake, D., Ridley, B., 2006. Halogen-driven low altitude O_3 and hydrocarbon losses in spring at northern high latitudes. Journal of Geophysical Research 111, D17313.